Journal of Dental Sciences 19 (2024) 1116–1125

Available online at www.sciencedirect.com

ScienceDirect

journal homepage: www.e-jds.com

Original Article

3D-bioprinted alginate-based bioink scaffolds with β-tricalcium phosphate for bone regeneration applications

Yi-Fan Wu [a,b], Ya-Ting Wen [c], Eisner Salamanca [a], Lwin Moe Aung [a], Yan-Qiao Chao [a], Chih-Yun Chen [d], Ying-Sui Sun [e*], Wei-Jen Chang [a,f**]

[a] School of Dentistry, College of Oral Medicine, Taipei Medical University, Taipei, Taiwan
[b] Department of Biomedical Engineering, Ming-Chuan University, Taoyuan, Taiwan
[c] Department of Medical Education, Taichung Veterans General Hospital, Taichung, Taiwan
[d] School of Oral Hygiene, College of Oral Medicine, Taipei Medical University, Taipei, Taiwan
[e] School of Dental Technology, College of Oral Medicine, Taipei Medical University, Taipei, Taiwan
[f] Dental Department, Shuang-Ho Hospital, Taipei Medical University, New Taipei, Taiwan

Received 22 December 2023; Final revision received 26 December 2023
Available online 12 January 2024

KEYWORDS
Alginate;
Beta-tricalcium phosphate (β-TCP);
Bioprinting;
Bone regeneration

Abstract *Background/purpose:* 3D-printed bone tissue engineering is becoming recognized as a key approach in dentistry for creating customized bone regeneration treatments fitting patients bone defects requirements. 3D bioprinting offers an innovative method to fabricate detailed 3D structures, closely emulating the native bone micro-environment and better bone regeneration. This study aimed to develop an 3D-bioprintable scaffold using a combination of alginate and β-tricalcium phosphate (β-TCP) with the Cellink® BioX printer, aiming to advance the field of tissue engineering.
Materials and methods: The physical and biological properties of the resulting 3D-printed scaffolds were evaluated at 10 %, 12 %, and 15 % alginate combined with 10 % β-TCP. The scaffolds were characterized through printability, swelling behavior, degradability, and element analysis. The biological assessment included cell viability, alkaline phosphatase (ALP) activity.
Results: 10 % alginate/β-TCP 3D printed at 25 °C scaffold demonstrated the optimal condition for printability, swelling capability, and degradability of cell growth and nutrient diffusion. Addition of β-TCP particles significantly improved the 3D printed material viscosity over only alginate ($P < 0.05$). 10 % alginate/β-TCP enhanced MG-63 cell's proliferation ($P < 0.05$) and alkaline phosphatase activity ($P < 0.001$).

* Corresponding author. School of Dental Technology, College of Oral Medicine, Taipei Medical University, No. 250 Wu-Hsing Street, Taipei, 11031, Taiwan.
** Corresponding author. School of Dentistry, College of Oral Medicine, Taipei Medical University, No. 250 Wu-Hsing Street, Taipei, 11031, Taiwan.
E-mail addresses: yingsuisun@tmu.edu.tw (Y.-S. Sun), cweijen1@tmu.edu.tw (W.-J. Chang).

https://doi.org/10.1016/j.jds.2023.12.023

Conclusion: This study demonstrated *in vitro* that 10 % alginate/β-TCP bioink characteristic for fabricating 3D acellular bioprinted scaffolds was the best approach. 10 % alginate/β-TCP bioink 3D-printed scaffold exhibited superior physical properties and promoted enhanced cell viability and alkaline phosphatase activity, showing great potential for personalized bone regeneration treatments.

Introduction

There is a growing need for more specific bone regeneration approaches due to the rising prevalence of bone defects in aging societies.[1] Bone grafting procedures have demanded annually more than two million graft procedures worldwide, which are among the most prevalent treatments.[2] Bone graft materials utilized in guided bone regeneration (GBR) treatment generally possess the biological property of osteoconduction or osteoinduction to promote or accelerate bone regeneration.[3] Unlike conventional methods that often struggle with creating complex geometries and ensuring consistent bioactivity, 3D bioprinting enables the precise fabrication of intricate 3D structures tailored to individual defect profiles. Synthetic 3D-printed bioink grafts predominate over some bone grafts when utilized as scaffolding for osteoconductive purposes. Their advantageous characteristics include mechanical properties, robust plasticity, and controllable degradation. Synthetic grafts do not demonstrate antigenic properties or the capacity to transmit diseases.[4,5]

3D-bioprinting is an emerging technique in bone tissue engineering and regenerative dentistry. It is hailed as a universal manufacturing method of the 21st century.[6] This technique offers a highly advanced, adaptable, and automated technology that surpasses conventional scaffold synthesis.[7] 3D bioprinting facilitates the swift creation of intricate 3D structures using computer models with diverse micro-architectures. Notably, 3D bioprinting can create tunnels within tissue structures, allowing for simultaneous material reabsorption and guided tissue regeneration.[8] In dentistry, biodegradable polymers have the potential to serve as graft materials in the bone regeneration process, as they may be molded to fit bone defects and expedite the production of new bone.[9] In instances involving technique bone defects, particularly those with two-wall or one-wall defects in guided tissue regeneration, using 3-D printed bioink materials can offer a tailored solution that ensures a precise fit for individualized patient treatment. Moreover, the utilization of bioactive 3-D printed customized form bone scaffolds can be beneficial in certain instances of horizontal or vertical ridge augmentation where there is an absence of a contained wall for the implantation of bone grafts. Successful 3D bioprinting depends on the ability of bioink to produce robust, high-resolution structures without compromising cell viability during or after printing. Thus, careful planning of material selection and printing conditions is essential for achieving bio-functionality at the site of tissue defects.[10] In the realm of biodegradable polymers for dental applications, 3D bioprinting has revolutionized the use of materials like collagen and alginate. When employed in 3D bioprinting, these natural materials offer distinct advantages over traditional bone graft materials. Collagen and alginate are two primary natural materials used in bioprinting. Both offer unique properties and biocompatibility.[11]. Alginate is particularly valued for its excellent gelation, biodegradability, and its role as a carrier for cell encapsulation and immobilization.[12] Collagen-containing hydrogels currently favored cell scaffolds and materials for tissue engineering, especially in cell interactions.[13]

Recent advancements in tissue engineering have emphasized using acellular bioinks, primarily composed of polycaprolactone (PCL) and polylactic acid (PLA) polymers, for creating porous scaffolds.[14,15] Incorporating bioceramic β-tricalcium phosphate (β-TCP) particles enhances these polymers' mechanical and biological properties.[16] β-TCP, a biodegradable and hydrophilic material, is preferable for bone healing due to its bioactivity.[17] Incorporating bioceramic β-TCP particles into these polymers enhances their mechanical strength and imbues them with bioactive properties crucial for bone healing. This approach addresses the critical limitations of traditional grafts, such as suboptimal porosity and mechanical strength, while ensuring biocompatibility and osteoconductivity. Studies have shown that acellular scaffolds can promote bone and cartilage regeneration without inducing inflammation or immune response.[18–20] Innovations in scaffold design, like Reed et al.'s high-compression alginate scaffold and Jung et al.'s chondrogenic environment scaffold,[21] demonstrate the versatility of acellular bioinks.[22] Rasperini et al.'s innovative method employs 3D-printed technologies with alginate, gelatin, and β-TCP to create a tailored graft that precisely conforms to the specific contours of bone defects, revolutionizing individualized treatment plans and periodontal regeneration.[23] These materials have broad potential in muscle tissue strengthening, wound healing, and osteochondral differentiation.[24] However, bioinks for bioprinting must align with criteria like biocompatibility and printability. Challenges remain, including the high melting temperatures of thermoplastic materials used in traditional 3D printing, which can affect biocompatibility. Other hurdles include limited cell availability, disease transmission risks, material selection, and the complexity and cost of manufacturing processes.[25]

While 3D-bioprinted scaffolds for bone regeneration represent a significant advancement in the field of tissue engineering, they are not without challenges that must be

addressed for their broader application and optimization. One of the primary concerns is the fine-tuning of scaffold properties, such as porosity and mechanical strength, to match the diverse requirements of different bone defect types. Additionally, ensuring consistent cell viability and proliferation within the printed structures remains complex, given the intricacies of cell-material interactions. Another challenge lies in scaling up the production of these scaffolds while maintaining quality and cost-effectiveness, a crucial factor for their widespread clinical adoption. Future research should focus on integrating advanced biofabrication techniques with novel bioactive materials to enhance the functionality of 3D-printed scaffolds. This includes exploring the incorporation of growth factors or angiogenic agents to promote faster tissue integration and regeneration.

Acellular scaffolds offer promising for optimizing host cell colonization and guiding tissue regeneration in dentistry. Natural biomaterials like alginate, used in these scaffolds, promote cell proliferation, adhesion, and differentiation, improving mechanical properties and architectural control. Despite evidence of alginate's long-term stability in animal models,[25,26] its impact on immune responses, such as inflammation, requires further investigation. Direct application of acellular extracellular matrix (ECM) components may induce a beneficial immunological response, facilitating tissue remodeling.[27,28] This study explores the use of alginate, gelatin, and β-TCP in developing a novel composite 3D-printed acellular scaffold for dental bone regeneration. Combining alginate's soft, cell-friendly matrix with the rigid, bone-mimicking structure of β-TCP creates a synergistic effect, enhancing the scaffold's overall performance in terms of mechanical support, biodegradability, and facilitation of osteoblast activity. This strategic choice of materials aims to overcome the limitations of traditional bone grafts, such as poor cell interaction and inadequate mechanical support, thereby aligning with our study's objective of developing a more effective solution for dental bone regeneration. The scaffold was crosslinked with calcium ions (Ca^{2+}) and evaluated for physical and biological properties at varying alginate concentrations (10 %, 12 %, 15 %) combined with β-TCP. The aim was to determine if higher alginate concentrations and β-TCP content enhance physical properties and promote cell viability and osteoblast differentiation. All materials complied with ICH Topic Q3C (R4) standards, ensuring the use of healthcare-grade polymers and non-toxic components.

Materials and methods

Bioink preparation and scaffold fabrication

To make the homogenous bioink, we prepared a gel solution with 4.5 % gelatin from bovine skin (Sigma Aldrich, St Louis, MO, USA), 10 % glycerol (>99 %, Sigma Aldrich), and varying concentrations of a specific type of sodium alginate (Mw: 12,000–400,000, Sigma Aldrich) in phosphate buffered saline (PBS) using a high-shear homogenizer.[29] This alginate was selected for its optimal viscosity and gelation properties, which are crucial for effective bioprinting. In addition, we also incorporated β-TCP particles (Sigma-Aldrich) (Molecular weight = 310.18 g/mol, particle size = 3–5 μm) into the base material to stimulate bone regeneration. The prepared bioink was then transferred into a 50 cc centrifuge tube for subsequent processing.

For the scaffold fabrication, the bioink was filled into a syringe and transferred into the printing cartridge with a 22 G nozzle of the BioX bioprinter (Cellink, Boston, MA, USA). A 10 cm dish was placed under the pneumatic printhead, and after adjusting the printing position and parameters, the bioprinting process began. The 3D layer square scaffolds (20 mm × 20 mm x 1 mm) were manufactured with a printing speed of 2 mm/s under 60–200 kPa of extrusion pressure, to optimize the scaffold structure.[30] After printing, the bioink scaffold was crosslinked with a 100 mM $CaCl_2$ solution for about 10 min before removal, ensuring structural integrity and stability before removal from the printing setup.[31,32]

Physical characterization

The bioink's viscosity was analyzed using a unidirectional shear rate and viscosity scan at various temperatures. A DV2THB viscometer (Brookfield, Middleboro, MA, USA) with SC4-14 cone spindle was used for these measurements. Surface micro-images and elemental analysis were conducted using a scanning electron microscope (SEM; Hitachi, Ltd., Tokyo, Japan) and energy-dispersive X-ray spectroscopy (EDS; Bruker Quantax, Germany) after the scaffolds were dried and coated with a thin gold layer. Similarly, functional group analysis was performed using Fourier-transform infrared spectroscopy (FTIR; Thermo Scientific, Waltham, MA, USA) with an attenuated total reflection (ATR) measurement kit.

The swelling rates of the bioink scaffolds were evaluated by weighing the scaffolds at different time points after immersion in a PBS solution at 37 °C for 6 h. The degradation rates were assessed similarly, but the scaffolds were immersed for a duration of 14 days.

Cell proliferation

Cell proliferation was evaluated using the AlamarBlue® Assay (Biosource International, Lewisville, TX, USA), which measures the metabolic activity of cells. MG-63 cells (5×10^4 cells/cm^2) were seeded onto the prepared scaffolds and cultured. The AlamarBlue reagent would change color and fluoresce when the reduction of the AlamarBlue reagent by metabolically active cells. This assay was performed at various time-points (1d, 3d, and 5d) to monitor cell proliferation, providing a quantitative measure of the scaffold's biocompatibility. The fluorescence intensity is directly proportional to the number of living cells on the bio-printed scaffolds by using a spectrophotometer.

Alkaline phosphatase activity

The alkaline phosphatase (ALP) activity, a biomarker of osteoblast activity and differentiation, was quantified using the Abcam ALP Assay Kit (ab83369) (Abcam, Cambridgeshire, UK). MG-63 cells (2.5×10^4 cells/cm^2) were seeded

onto the scaffolds and cultured in osteogenic differentiation media. The substrate p-nitrophenylphosphate (pNNP) was added, which ALP hydrolyzes to release phosphate. The absorbance was measured at 405 nm using a spectrophotometer. Bone cell differentiation on the bioprinted scaffold was measured after 1 day, 3 days, and 5 days.

Statistical analyses

The data were presented as the mean and standard deviation (SD). Each experimental data was replicated at least three times using different samples in each group. Statistical significance was determined using a two-tailed T-test, with $^{*}P$-value <0.05 and $^{**}P$-value <0.01 as statistical significance.

Result

Viscosity properties of alginate-based bioinks

As shown in Fig. 1, An increase in temperature from 25 to 40 °C enhanced the curve of the shear-viscosity property of the bioinks. This temperature increase also leads to decreased viscosity in Pa·s. similar to gelatin–methacrylamide/hyaluronic acid–methacrylate (GelMa/HAMa) hydrogel tendency when 3D printed.[33] However, beyond a shear rate of 50 s^{-1}, the viscosity curves tended to plateau, indicating the onset of shear-thinning behavior for this hydrogel bioink.

Fabrication of 3D bioprinted constructs

To assess the printability and geometric fidelity of the hybrid bioinks based on the prior rheological evaluation, all of the condition samples were loaded to print a 3D grid-like structure scaffold. As depicted in Fig. 2, samples were printed under optimal gelation condition, smooth and uniform filaments were extruded continuously, leading to a standard grid construct with high fidelity. Notably, samples mixed with β-TCP displayed distinct color changes and dimensional stability. In the proper-gelation conditions, smooth and uniform filaments were extruded continuously, resulting in a standard grid construct with obviously distinguished changes in color in the samples mixed with β-TCP.[34] This indicates high fidelity, good printing accuracy and dimensional stability. The physicochemical and biological assessments of these constructs showed in subsequent sections.

Surface morphological and element characterizations by scanning electron microscope and energy-dispersive X-ray spectroscopy

The homogeneous distribution of β-TCP within the filaments was observed in the SEM images in Fig. 3, similar to the non-fibrillar homogeneous modular hyaluronan-based hydrogel structure obtained after using the same 3D printer.[35] Notably, the addition of β-TCP into the alginate bioink led to more roughness on the scaffold surfaces than alginate alone. This suggests a uniform dispersion of β-TCP within the alginate-based hydrogel matrix, adding advantages such as biological activity and similarity to the mineral phase of human bone.[9,36] Due to the rough surface of the β-TCP scaffolds, adding this biomaterial with hydrogels may promote effective cell adhesion and deliver necessary nutrients into the surgical area where bone tissue regeneration will be done.

Element distribution was further analyzed with EDS. The concentrations of elements were similar in the only alginate scaffold samples in the EDS results, Carbon (C) and oxygen (O) were dominant in alginate scaffold samples. By comparison, calcium (Ca) and phosphorous (P) were only detected alginate/β-TCP scaffold. It verifies that these particles originate from the addition of β-TCP (Table 1).

Structure analysis by fourier-transform infrared spectroscopy

In Fig. 4, the primary characteristic transmittance peaks for alginate were observed at approximately 1640 cm^{-1}, attributing to the overlapped asymmetric stretching vibration of COO^{-}, the stretching vibration of –C–N groups, C=O stretching asymmetric stretching, and amide I.[37–39] The β-TCP exhibited peaks within the range of 950∼1150 cm^{-1}, corresponding to the vibrational mode of PO_4^{3-}.[40] In the alginate/β-TCP fibers, the peaks merged with those of

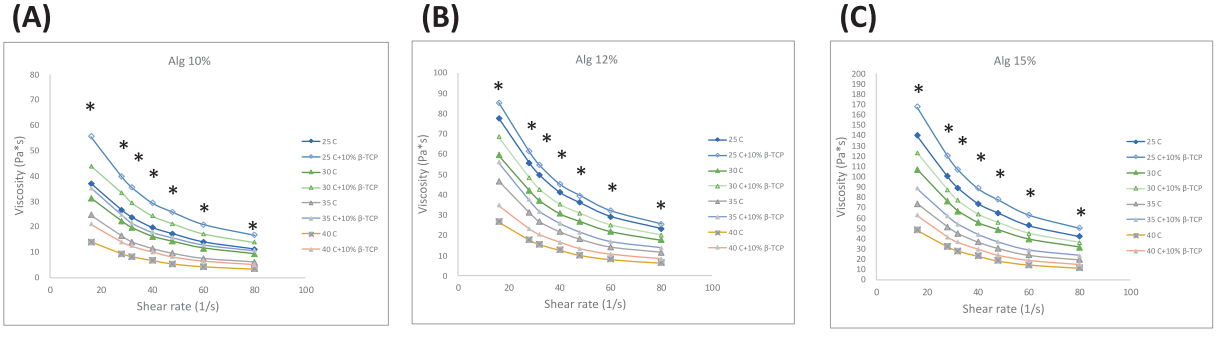

Figure 1 Rheological properties of alginate-based bioinks at concentrations of (A) 10 wt%, (B) 12 wt% and (C) 15 wt%. The viscosity is plotted over a shear rate from 15 s^{-1} to 80 s^{-1}, demonstrating the shear-thinning behavior of the bioinks. At the same alginate concentration, the addition of β-TCP to the bioink had a statistically significant difference compared to bioink without β-TCP ($P < 0.05$) at the low shear rate region. β-TCP: β-tricalcium phosphate.

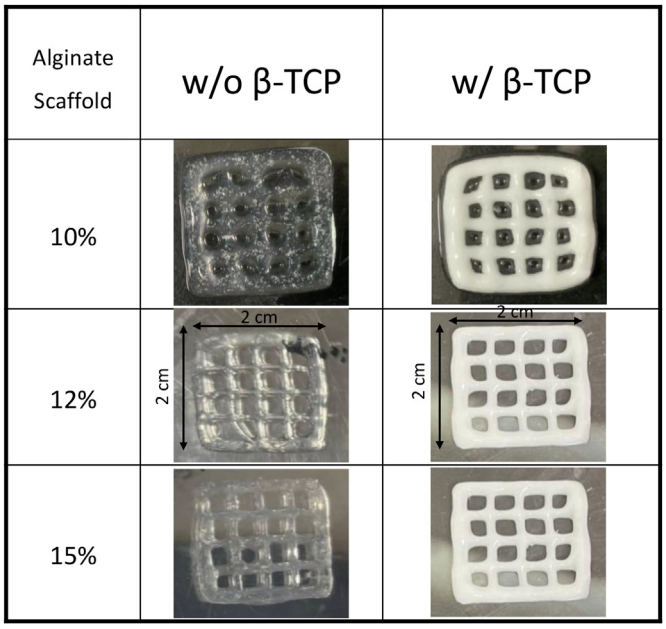

Figure 2 Macroscopic images of 3D-printed at different alginate concentrations, alginate alone or alginate/β-TCP (dimensions: 2 cm*2 cm). Images depict the geometry immediately after printing and after undergoing a 10-min cross-linking process in a $CaCl^2$ bath. β-TCP: β-tricalcium phosphate.

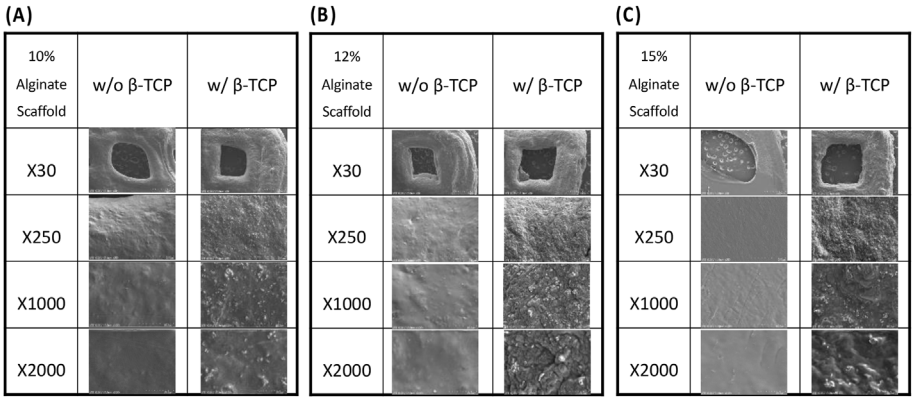

Figure 3 SEM images of 3D-printed scaffolds at different alginate concentrations: (A) 10, (B) 12, (C) 15 wt%, alginate, and alginate/β-TCP particles. Images are presented at four different magnifications (X30, X250, X1000, X2000) to highlight structural details. SEM: Scanning Electron Microscope; β-TCP: β-tricalcium phosphate.

Table 1 Element distribution of alginate-based scaffolds without and with β-TCP particles from EDS analysis. β-TCP: β-tricalcium phosphate; EDS: Energy-dispersive X-ray spectroscopy.

Element (wt.%)	Alginate scaffold 10 %		Alginate scaffold 12 %		Alginate scaffold 15 %	
	w/o β-TCP	w/β-TCP	w/o β-TCP	w/β-TCP	w/o β-TCP	w/β-TCP
C	43.81	41.61	43.02	38.07	44.10	41.87
O	44.39	40.58	45.84	42.46	44.81	43.04
Na	3.40	3.00	3.04	2.77	3.11	3.37
Cl	1.48	2.62	1.13	2.39	1.91	1.54
Ca	1.37	8.60	1.29	7.65	1.68	6.76
P	—	3.60	—	3.06	—	3.05

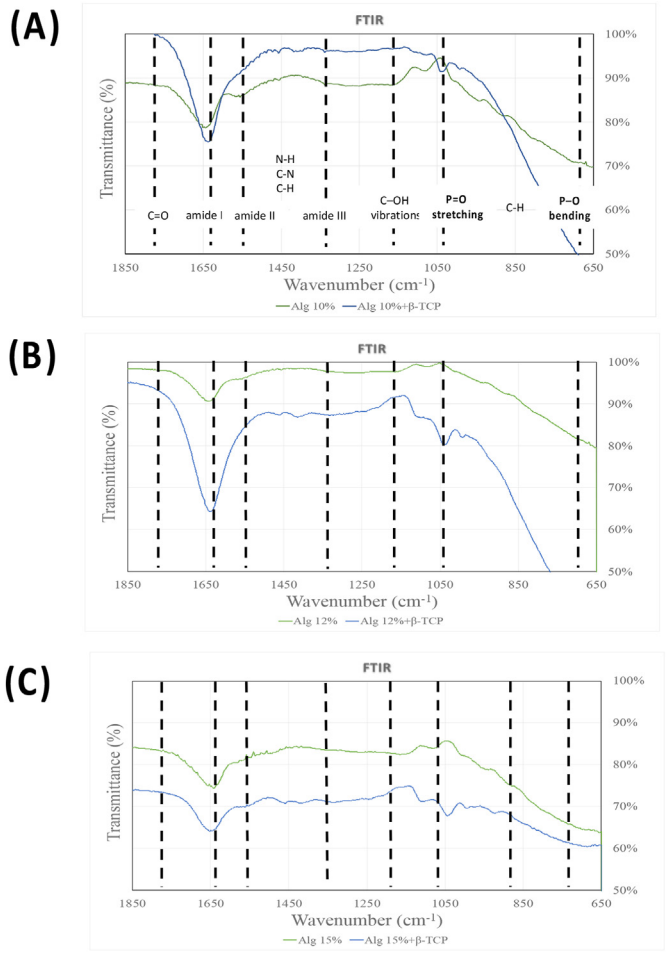

Figure 4 FTIR: Fourier-transform infrared spectroscopy spectra of the bioprinting scaffold and its individual components. (A) Alg 10 % and Alg 10 %+β-TCP (B) Alg 12 % and Alg 12 %+β-TCP (C) Alg 15 % and Alg 15 %+β-TCP. FTIR: Fourier-Transform Infrared Spectroscopy.

alginate, with a noticeable shift occurring within the 950∼1150 cm^{-1} range (P═O stretching) and ∼600 cm^{-1} (P—O) upon the addition of β-TCP particles.[41] The slight peak at ∼ 1420 cm^{-1} in both groups represented the symmetric stretching vibration of the COO groups. However, the C—NH^{2+} stretching vibration peak at approximately 1510 cm^{-1} disappeared in all bioink samples.

Swelling behavior and degradability

The swelling behavior of the bioprinted constructs is illustrated in Fig. 5(A) and **(B)**. All scaffolds exhibited rapid swelling with a 1.4—1.9-fold increase within the first hour. The scaffolds then reached a stable equilibrium after approximately 6 h.[42] Notably, scaffolds without β-TCP groups swelled more than hydrogels containing β-TCP particles.

The assessment of scaffold behavior and its impact on cellular differentiation needs the inclusion of degradation tests.[42] The degradation of the constructs is depicted in Fig. 5(C) and **(D)**. There were no significant changes in degradation for the alginate scaffolds of different concentrations. However, in the case of the alginate/β-TCP groups, a significant increase in construct degradation was observed as the alginate concentration increased. Notably, the constructs composed of 10 % alginate with β-TCP demonstrated superior stability, exhibiting only around 5 % degradation in PBS over a period of 14 days, compared to the other samples.

Cell viability for biological assessment

The result of the AlamarBlue assay, shown in Fig. 6, provides an assessment of metabolic activity and proliferation of the cells within the scaffolds. A *t*-test analysis revealed a statistically significant increase in cell activity for the alginate/β-TCP scaffolds ($P < 0.05$) compared to the pure alginate scaffolds at a 10 % concentration on Day 5. As indicated by a *t*-test, this increase was statistically significant, potentially attributable to the higher viscosity and inorganic component of the alginate/β-TCP mixture. However, no significant differences were observed in cell activity across different alginate concentrations on Day 1 and Day 3 of the culture.

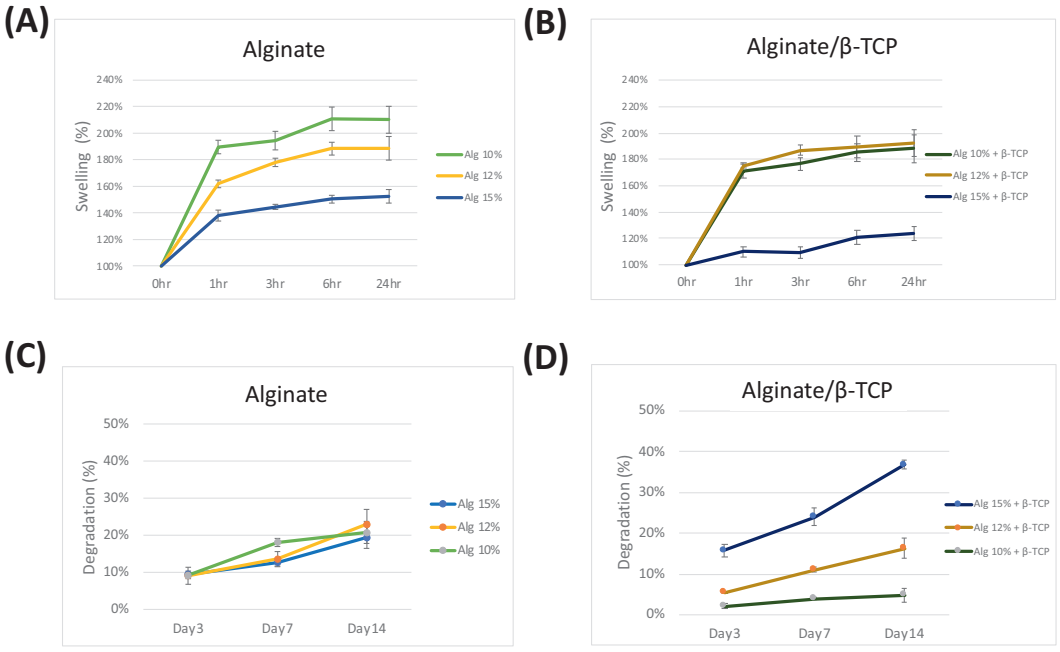

Figure 5 The swelling ratio of 3D bio-printed constructs derived from **(A)** alginate and **(B)** alginate/β-TCP scaffolds. Degradation of constructs from alginate **(C)** and alginate/β-TCP **(D)** scaffolds. Data are presented as mean ± standard deviation (n = 3).

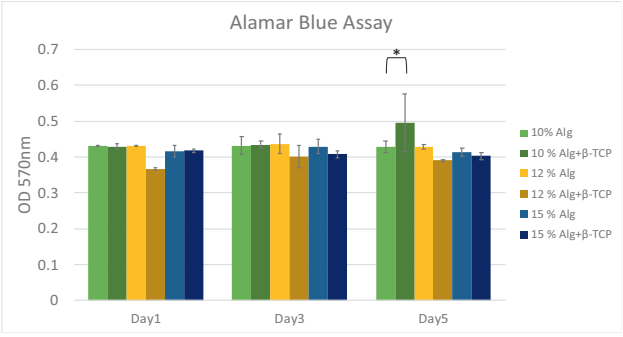

Figure 6 MG-63 viability by alamar blue assay in alginate and alginate/β-TCP scaffolds. Percentage of living cells in the 3D printed scaffold at days 1, 3, and 5. (* T-test; $P < 0.05$). β-TCP: β-tricalcium phosphate.

Alkaline phosphatase activity

As illustrated in Fig. 7, the 10 % alginate/β-TCP group had the highest ALP activity on Day 5, with a mean ALP activity of 27 nmol/well, significantly surpassing than other groups on Days 3 and 5 ($P < 0.001$). Additionally, scaffolds 3D printed with β-TCP particles showed superior to those composed of only alginate-based scaffolds, particularly on Day 5 ($P < 0.05$), promoting osteogenic differentiation of MG-63 cells *in vitro*, similar to previous results.[43] This trend suggests a pronounced effect of β-TCP in promoting osteogenic differentiation of MG-63 cells *in vitro*. Across all groups, ALP activities increased with culture time throughout the measurement periods, indicating successful cell differentiation.

Discussion

Integrating β-TCP with alginate in 3D printing offers a promising avenue for creating advanced biomaterials tailored to specific patient needs. Subsequently, the physical and biological assessments will contribute to the advancement of innovative 3D-printed biomaterials and their application for customized bone regeneration. Alginate is a natural polysaccharide that effectively mimics the extracellular matrix of tissues and is frequently utilized in 3D bioprinting for its capacity to form hydrogels, which are ideal for the printing process.[44] β-TCP provides mechanical support due to its ceramic nature, which is important for applications in bone regeneration. Besides, it has a composition similar to the mineral component of bone, and in combination with alginate can offer additional structural integrity and results in a biomimetic 3D printed composite scaffold.[17]

The printing quality for 3D printed components is contingent upon the viscosity of the material, hence establishing viscosity as a pivotal metric to assess in 3D printing procedures. Fig. 1 presents the viscosity and shear rate relationship for six different bioink formulations at varying temperatures. It was observed that bioinks with a higher alginate concentration exhibited increased viscosity. Furthermore, adding β-TCP (Alginate/β-TCP) into the bioink amplified its viscosity properties at equivalent alginate concentrations with statistically significant differences. SEM was utilized to examine the pore structure and microstructure of the hydrogel scaffolds. As depicted in Figs. 2 and 3, increased in alginate concentration within the bioink composition resulted in denser surface structures with smaller cavities and pores, finally forming a smoother

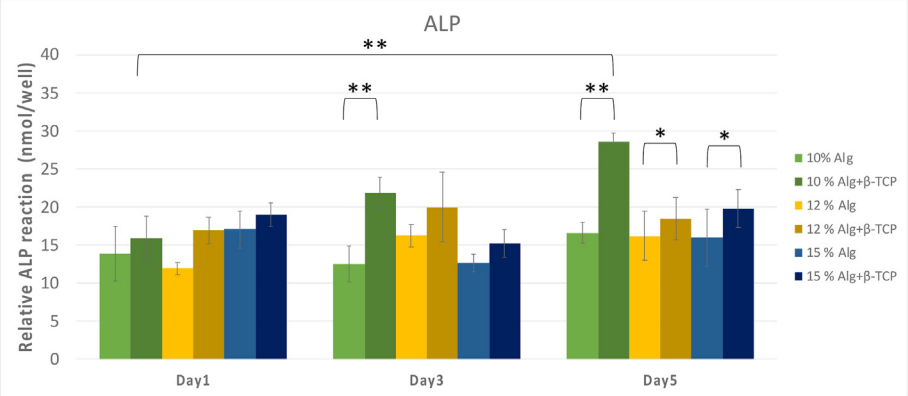

Figure 7 Alkaline phosphatase (ALP) activity of different concentrations of alginate/β-TCP and alginate scaffolds. The 10 % alginate/β-TCP scaffolds had superior ALP activity results than others. β-TCP: β-tricalcium phosphate.

surface. Both 3D printed scaffolds exhibited comparable grid area and aspect ratio, similar to previous results using the same Bioink 3D printer.[42] These findings also suggest that the incorporation of β-TCP did not have a substantial impact on the printability of alginate. β-TCP is known to stimulate osteogenesis, the process of bone formation. Combining it with alginate can create a synergistic effect, potentially promoting a favorable environment for bone cell activity and differentiation.[17]

The functional group structures of alginate and alginate/β-TCP scaffolds were analyzed using FTIR spectroscopy. Fig. 4 demonstrated the prominent peaks for each scaffold fiber at different alginate concentrations. Due to PBS absorption by the hydrogel, attributable to its hydrophilic skeleton and porous structure, each scaffold undergoes a swift enlargement. Then, uptake increased over time approximately 6 h until a constant equilibrium was achieved. According to the available reports,[45] the swelling values of scaffold exhibit a decrease due to their compact internal structure. Hence, the reduced water absorption seen in the scaffolds incorporating β-TCP can be attributed to the elevated viscosity of the bioink, relative to that of Alginate alone. Meanwhile, the swelling percentage was inversely related to alginate concentration. The higher water retention capacity indicates the scaffold's potential to serve as a nutrient reserve for cells at the bone defect site. Thus, both 10 % and 12 % alginate with and without β-TCP particles had better swelling properties than 15 %.

Ideally, a bioink should possess the properties of printability, biodegradability, and biocompatibility with cells.[46] Both alginate and β-TCP are known for their biocompatibility. Combining these materials enhances the overall biocompatibility of the composite, making it suitable for use in biological systems without triggering adverse reactions.[47,48] The results from cell viability assessment also suggest that alginate/β-TCP scaffolds can support a sufficient number of viable cells, thereby potentially facilitating optimal bone regeneration due to their superior physical properties. While our previous studies have suggested that the beneficial effects of β-TCP incorporation should become more pronounced over time.[9,49,50] β-TCP is widely used in clinical interventions for its notable features including biocompatibility, osteoconductivity, osteoinductivity, and biodegradability.[43] The physical properties of scaffolds like swelling and degradation behavior are also critical in assessing their suitability for long-term bone regeneration applications. Alkaline phosphatase (ALP) activity is associated with the early stages of bone matrix mineralization. It is a crucial indicator for osteoblast differentiation and can predict subsequent bone formation.[51]

Alginate-based bioink scaffold produced by 3D printing technology brings several advantages, including desirable optimal scaffold architecture and customized printability, enhanced tissue mimicry, and improved biological and physical properties. For example, combining alginate with β-TCP allows for creating complex 3D structures, which provides a platform for precise and personalized fabrication. This bioprinted structure can be designed to have optimal porosity and permeability, facilitating nutrient and oxygen diffusion throughout the scaffold.[52,53] Moreover, incorporating bioresorbable β-TCP ensures that the scaffold gradually degrades over time, allowing for the natural integration of newly formed bone tissue. This property aligns for future usage with the principles of guided tissue regeneration and guided bone regeneration. Degradation rate data shows that 10%Alg+ β-TCP resorption at 14 days is only around 5 %, aligns with the principles of GBR, allowing for the natural integration of newly formed bone tissue. The 3D-printed scaffold serves as a substrate for cells involved in bone regeneration. It provides a structured environment for cell attachment, migration, and the formation of new bone tissue. This is critical for supporting cell viability and tissue regeneration. This biomimicry can support cellular adhesion, proliferation, and tissue regeneration.[54] In clinical dentistry, it is expected that the application of 3D bioprinted alginate-β-TCP scaffolds will be relevant for enhancing bone regeneration not only around the teeth but also around the dental implants. It aids particularly in improved osteoblast-like cell response and regeneration of bone, which provide a stable and supportive foundation for implant placement. Furthermore, the combination of alginate and β-TCP can be advantageous for creating dental implants or scaffolds with tailored properties. The biomaterial composite can be adapted to the specific requirements of dental

applications, supporting the regeneration of bone tissues around dental implants.

3D-printed acellular alginate-based scaffolds are still new and innovative. Ongoing research in this field aims to further optimize the properties of 3D-printed alginate-β-TCP scaffolds, with the potential for clinical applications in diverse scenarios requiring guided bone regeneration.[55,56] The combination of alginate and β-TCP opens avenues for research and innovation in the field of tissue engineering and regenerative medicine. Researchers can explore various formulations and ratios to optimize the composite for specific applications. It's important to note that the success of combining alginate and β-TCP depends on the specific application, the intended use, and the desired properties of the biomaterial composite. Additionally, thorough research testing and validation are necessary to ensure the safety and efficacy of the combined materials for clinical applications. In summary, the application of 3D bioprinted alginate-β-TCP in guided bone regeneration holds great promise for enhancing the precision, effectiveness, and versatility of bone regeneration procedures, particularly in dental and orthopedic contexts. The combination of biocompatible materials and advanced printing technology represents a significant stride in the field of regenerative medicine.

The integration of β-TCP into the 10 % alginate bioink, 3D-printed at 25 °C, exhibited advantageous characteristics in relation to printability, swelling, and degradability. This optimal alginate/β-TCP scaffold exhibit optimal porosity and mechanical strength, essential for maintaining space and providing structural support during the critical early stages of bone healing and regeneration around dental implants. The importance of β-TCP viscosity was observed in its role in enabling the growth and proliferation of bone cells, as well as supporting the osteogenic cell's differentiation. The cost-effectiveness application of this acellular bioink offers a feasible method for attaining personalized bone regeneration, and bolstering for its possible implementation in intrabony defect regeneration procedures. Despite the promising results observed in the physical and biological assessments of our 3D-printed alginate-β-TCP scaffolds, it is imperative to consider the immunological implications of these biomaterials when considering use in the body. Therefore, future investigations should prioritize examining the immunological response and potential inflammatory reactions these scaffolds elicit to ensure their safety and effectiveness for clinical applications.

Declaration of competing interest

The authors declare that there are no conflicts of interest regarding the publication of this paper.

Acknowledgments

This study was supported by grants from National Science and Technology Council (NSTC) [Grant number: 110-2314-B-038-065-MY3, 112-2221-E-038-006-MY3], National Taiwan University of Science and Technology-Taipei Medical University Joint Research Program [Grant number: 112-TMU-NTUST-112-02], Wan Fang Hospital-Taipei Medical University Program [Grant Number: 111 TMU-WFH-20, 112 TMU-WFH-26], and Collaboration project between National Taiwan University Hospital and Taipei Medical University [Grant number: 111-TMU06].

References

1. Bose S, Roy M, Bandyopadhyay A. Recent advances in bone tissue engineering scaffolds. *Trends Biotechnol* 2012;30:546–54.
2. Giannoudis PV, Dinopoulos H, Tsiridis E. Bone substitutes: an update. *Injury* 2005;36:S20–7.
3. LeGeros R, Lin S, Rohanizadeh R, et al. Biphasic calcium phosphate bioceramics: preparation, properties and applications. *J Mater Sci Mater Med* 2003;14:201–9.
4. Causa F, Netti PA, Ambrosio L, et al. Poly-ϵ-caprolactone/hydroxyapatite composites for bone regeneration: in vitro characterization and human osteoblast response. *J Biomed Mater Res* 2006;76:151–62.
5. Chuenjitkuntaworn B, Inrung W, Damrongsri D, et al. Polycaprolactone/hydroxyapatite composite scaffolds: preparation, characterization, and in vitro and in vivo biological responses of human primary bone cells. *J Biomed Mater Res* 2010;94:241–51.
6. Mallakpour S, Azadi E, Hussain CM. State-of-the-art of 3D printing technology of alginate-based hydrogels: an emerging technique for industrial applications. *Adv Colloid Interface Sci* 2021;293:102436.
7. Xu X, Jha AK, Harrington DA, et al. Hyaluronic acid-based hydrogels: from a natural polysaccharide to complex networks. *Soft Matter* 2012;8:3280–94.
8. Schieker M, Seitz H, Drosse I, et al. Biomaterials as scaffold for bone tissue engineering. *Eur J Trauma Emerg Surg* 2006;32:114–24.
9. Salamanca E, Tsao T-C, Hseuh H-W, et al. Fabrication of polylactic acid/β-tricalcium phosphate FDM 3D printing fiber to enhance osteoblastic-like cell performance. *Front Mater* 2021;8:683706.
10. Decante G, Costa JB, Silva-Correia J, et al. Engineering bioinks for 3D bioprinting. *Biofabrication* 2021;13:032001.
11. Labowska MB, Michalak I, Detyna J. Methods of extraction, physicochemical properties of alginates and their applications in biomedical field - a review. *Open Chem* 2019;17:738–62.
12. Datta S, Barua R, Das J. Importance of alginate bioink for 3D bioprinting in tissue engineering and regenerative medicine. In: *Alginates - recent uses of this natural polymer*. IntechOpen, 2019.
13. Frantz C, Stewart KM, Weaver VM. The extracellular matrix at a glance. *J Cell Sci* 2010;123:4195–200.
14. Sherwood JK, Riley SL, Palazzolo R, et al. A three-dimensional osteochondral composite scaffold for articular cartilage repair. *Biomaterials* 2002;23:4739–51.
15. Hutmacher DW, Schantz T, Zein I, et al. Mechanical properties and cell cultural response of polycaprolactone scaffolds designed and fabricated via fused deposition modeling. *J Biomed Mater Res* 2001;55:203–16.
16. Yang F, Both SK, Yang X, et al. Development of an electrospun nano-apatite/PCL composite membrane for GTR/GBR application. *Acta Biomater* 2009;5:3295–304.
17. Bohner M, Santoni BLG, Döbelin N. β-tricalcium phosphate for bone substitution: synthesis and properties. *Acta Biomater* 2020;113:23–41.
18. Sadtler K, Wolf MT, Ganguly S, et al. Divergent immune responses to synthetic and biological scaffolds. *Biomaterials* 2019;192:405–15.
19. Zhang S, Hu B, Liu W, et al. Articular cartilage regeneration: the role of endogenous mesenchymal stem/progenitor cell

recruitment and migration. *Semin Arthritis Rheum* 2020;50:198–208.
20. Im G-I. Endogenous cartilage repair by recruitment of stem cells. *Tissue Eng Part B* 2016;22:160–71.
21. Reed S, Lau G, Delattre B, et al. Macro-and micro-designed chitosan-alginate scaffold architecture by three-dimensional printing and directional freezing. *Biofabrication* 2016;8:015003.
22. Jung CS, Kim BK, Lee J, et al. Development of printable natural cartilage matrix bioink for 3D printing of irregular tissue shape. *Tissue Eng Regen Med* 2018;15:155–62.
23. Rasperini G, Pilipchuk S, Flanagan C, et al. 3D-printed bioresorbable scaffold for periodontal repair. *J Dent Res* 2015;94.153S-7S.
24. Gao G, Yonezawa T, Hubbell K, et al. Inkjet-bioprinted acrylated peptides and PEG hydrogel with human mesenchymal stem cells promote robust bone and cartilage formation with minimal printhead clogging. *Biotechnol J* 2015;10:1568–77.
25. Vanden Berg-Foels WS. In situ tissue regeneration: chemoattractants for endogenous stem cell recruitment. *Tissue Eng Part B* 2014;20:28–39.
26. Shkand TV, Chizh MO, Sleta IV, et al. Assessment of alginate hydrogel degradation in biological tissue using viscosity-sensitive fluorescent dyes. *Methods Appl Fluoresc* 2016;4:044002.
27. Sirlin CB, Brossmann J, Boutin RD, et al. Shell osteochondral allografts of the knee: comparison of MR imaging findings and immunologic responses. *Radiology* 2001;219:35–43.
28. Fraitzl CR, Egli RJ, Wingenfeld C, et al. Time course of biological activity in fresh murine osteochondral allografts paralleled to the recipient's immune response. *J Invest Surg* 2008;21:109–17.
29. Zhang J, Wehrle E, Vetsch JR, et al. Alginate dependent changes of physical properties in 3D bioprinted cell-laden porous scaffolds affect cell viability and cell morphology. *Biomed Mater* 2019;14:065009.
30. Lin YH, Chiu YC, Shen YF, et al. Bioactive calcium silicate/poly-ε-caprolactone composite scaffolds 3D printed under mild conditions for bone tissue engineering. *J Mater Sci Mater Med* 2018;29:1–13.
31. Ávila HM, Schwarz S, Rotter N, et al. 3D bioprinting of human chondrocyte-laden nanocellulose hydrogels for patient-specific auricular cartilage regeneration. *Bioprinting* 2016;1:22–35.
32. Müller M, Öztürk E, Arlov Ø, et al. Alginate sulfate–nanocellulose bioinks for cartilage bioprinting applications. *Ann Biomed Eng* 2017;45:210–23.
33. D O'Connell C, Di Bella C, Thompson F, et al. Development of the Biopen: a handheld device for surgical printing of adipose stem cells at a chondral wound site. *Biofabrication* 2016;8:015019.
34. Ouyang L, Yao R, Zhao Y, et al. Effect of bioink properties on printability and cell viability for 3D bioplotting of embryonic stem cells. *Biofabrication* 2016;8:035020.
35. Matthiesen I, Jury M, Rasti Boroojeni F, et al. Astrocyte 3D culture and bioprinting using peptide functionalized hyaluronan hydrogels. *Sci Technol Adv Mater* 2023;24:2165871.
36. Takagi T, Aoki A, Ichinose S, et al. Effective removal of calcified deposits on microstructured titanium fixture surfaces of dental implants with erbium lasers. *J Periodontol* 2018;89:680–90.
37. Dong Z, Wang Q, Du Y. Alginate/gelatin blend films and their properties for drug controlled release. *J Membr Sci* 2006;280:37–44.
38. Han J, Zhou Z, Yin R, et al. Alginate–chitosan/hydroxyapatite polyelectrolyte complex porous scaffolds: preparation and characterization. *Int J Biol Macromol* 2010;46:199–205.
39. Sarmento B, Ferreira D, Veiga F, et al. Characterization of insulin-loaded alginate nanoparticles produced by ionotropic pre-gelation through DSC and FTIR studies. *Carbohydr Polym* 2006;66:1–7.
40. Chen Y, Xiong X, Liu X, et al. 3D Bioprinting of shear-thinning hybrid bioinks with excellent bioactivity derived from gellan/alginate and thixotropic magnesium phosphate-based gels. *J Mater Chem B* 2020;8:5500–14.
41. Siddiqui N, Pramanik K, Jabbari E. Osteogenic differentiation of human mesenchymal stem cells in freeze-gelled chitosan/nano β-tricalcium phosphate porous scaffolds crosslinked with genipin. *Mater Sci Eng C* 2015;54:76–83.
42. Lafuente-Merchan M, Ruiz-Alonso S, Espona-Noguera A, et al. Development, characterization and sterilisation of Nanocellulose-alginate-(hyaluronic acid)-bioinks and 3D bioprinted scaffolds for tissue engineering. *Mater Sci Eng C* 2021;126:112160.
43. Jiao X, Sun X, Li W, et al. 3D-printed β-tricalcium phosphate scaffolds promote osteogenic differentiation of bone marrow-deprived mesenchymal stem cells in an N6-methyladenosine-dependent manner. *Int J Bioprint* 2022;8:31–44.
44. Neves MI, Moroni L, Barrias CC. Modulating alginate hydrogels for improved biological performance as cellular 3D microenvironments. *Front Bioeng Biotechnol* 2020;8:665.
45. Yu F, Cao X, Li Y, et al. Diels–Alder crosslinked HA/PEG hydrogels with high elasticity and fatigue resistance for cell encapsulation and articular cartilage tissue repair. *Polym Chem* 2014;5:5116–23.
46. Xu LP, Meng J, Zhang S, et al. Amplified effect of surface charge on cell adhesion by nanostructures. *Nanoscale* 2016;8:12540–3.
47. Kang HJ, Makkar P, Padalhin AR, et al. Comparative study on biodegradation and biocompatibility of multichannel calcium phosphate based bone substitutes. *Mater Sci Eng C* 2020;110:110694.
48. Urruela-Barrios R, Ramírez-Cedillo E, Díaz de León A, et al. Alginate/gelatin hydrogels reinforced with TiO2 and β-TCP fabricated by microextrusion-based printing for tissue regeneration. *Polymers* 2019;11:457.
49. Ngo ST, Lee WF, Wu YF, et al. Fabrication of solvent-free PCL/β-TCP composite fiber for 3D printing: physiochemical and biological investigation. *Polymers* 2023;15:1391.
50. Salamanca E, Pan YH, Sun YS, et al. Magnesium modified β-tricalcium phosphate induces cell osteogenic differentiation in vitro and bone regeneration in vivo. *Int J Mol Sci* 2022;23:1717.
51. Vimalraj S. Alkaline phosphatase: structure, expression and its function in bone mineralization. *Gene* 2020;754:144855.
52. Yazdanpanah Z, Johnston JD, Cooper DM, et al. 3D bioprinted scaffolds for bone tissue engineering: state-of-the-art and emerging technologies. *Front Bioeng Biotechnol* 2022;10:824156.
53. Lutzweiler G, Ndreu Halili A, Engin Vrana N. The overview of porous, bioactive scaffolds as instructive biomaterials for tissue regeneration and their clinical translation. *Pharmaceutics* 2020;12:602.
54. Ashammakhi N, Ahadian S, Xu C, et al. Bioinks and bioprinting technologies to make heterogeneous and biomimetic tissue constructs. *Mater Today Bio* 2019;1:100008.
55. Gungor-Ozkerim PS, Inci I, Zhang YS, et al. Bioinks for 3D bioprinting: an overview. *Biomater Sci* 2018;6:915–46.
56. Chen X, Anvari-Yazdi AF, Duan X, et al. Biomaterials/bioinks and extrusion bioprinting. *Bioact Mater* 2023;28:511–36.